TISSUE ENGINEERING: Part C
Volume 17, Number 6, 2011

DOI: 10.1089/ten.tec.2010.0698

A Whole-Organ Regenerative Medicine Approach for Liver Replacement

Alejandro Soto-Gutierrez, M.D., Ph.D.,[1,2,*] Li Zhang, M.D., M.S.,[2,3,*] Chris Medberry, B.S.,[2,3] Ken Fukumitsu, M.D., Ph.D.,[1,2] Denver Faulk, B.S.,[2,3] Hongbin Jiang, M.D.,[2,3] Janet Reing, M.S.,[2,3] Roberto Gramignoli, Ph.D.,[4] Junji Komori, M.D., Ph.D.,[2,4] Mark Ross, Ph.D.,[4,5] Masaki Nagaya, M.D., Ph.D.,[1,2] Eric Lagasse, Ph.D.,[2,4] Donna Stolz, Ph.D.,[4,5] Stephen C. Strom, Ph.D.,[4] Ira J. Fox, M.D.,[1,2] and Stephen F. Badylak, D.V.M., Ph.D., M.D.[2,3,6]

Background & Aims: The therapy of choice for end-stage liver disease is whole-organ liver transplantation, but this option is limited by a shortage of donor organs. Cell-based therapies and hepatic tissue engineering have been considered as alternatives to liver transplantation, but neither has proven effective to date. A regenerative medicine approach for liver replacement has recently been described that includes the use of a three-dimensional organ scaffold prepared by decellularization of xenogeneic liver. The present study investigates a new, minimally disruptive method for whole-organ liver decellularization and three different cell reseeding strategies to engineer functional liver tissue.

Methods: A combination of enzymatic, detergent, and mechanical methods are used to remove all cells from isolated rat livers. Whole-organ perfusion is used in a customized organ chamber and the decellularized livers are examined by morphologic, biochemical, and immunolabeling techniques for preservation of the native matrix architecture and composition. Three different methods for hepatocyte seeding of the resultant three-dimensional liver scaffolds are evaluated to maximize cell survival and function: (1) direct parenchymal injection, (2) multistep infusion, or (3) continuous perfusion.

Results: The decellularization process preserves the three-dimensional macrostructure, the ultrastructure, the composition of the extracellular matrix components, the native microvascular network of the liver, and the bile drainage system, and up to 50% of growth factor content. The three-dimensional liver matrix reseeded with the multistep infusion of hepatocytes generated ~90% of cell engraftment and supported liver-specific functional capacities of the engrafted cells, including albumin production, urea metabolism, and cytochrome P450 induction.

Conclusions: Whole-organ liver decellularization is possible with maintenance of structure and composition suitable to support functional hepatocytes.

Introduction

Liver disease is the 11th leading cause of mortality in the United States and results in over 25,000 deaths annually.[1] Allogenic liver transplantation represents the treatment of choice for end-stage liver disease, but the shortage of donor organs and high cost are both limiting factors.[2] In spite of the tremendous *in vivo* regenerative capacity of the native healthy liver, hepatocytes have proven recalcitrant to *in vitro* expansion or maintenance of a functional phenotype in culture. *In vitro* culture of hepatocytes is routinely associated with de-differentiation and decreased hepatocyte-specific functions even in the best of the cases.[3] Several approaches have been investigated to retain the proliferation capacity and functionality of hepatocytes *ex vivo*—none with sustained success. Recent studies have shown that decellularization of whole organs such as livers,[4] lung,[5,6] and heart[7,8] are possible, but the methods used have typically included

[1]Transplantation Section, Department of Surgery, Children's Hospital of Pittsburgh, Center for Innovative Regenerative Therapies, University of Pittsburgh, Pittsburgh, Pennsylvania.
[2]McGowan Institute for Regenerative Medicine, Pittsburgh, Pennsylvania.
Departments of [3]Bioengineering and [4]Pathology, University of Pittsburgh, Pittsburgh, Pennsylvania.
[5]Center for Biologic Imaging, University of Pittsburgh Medical School, Pittsburgh, Pennsylvania.
[6]Department of Surgery, University of Pittsburgh, Pittsburgh, Pennsylvania.
*These two authors contributed equally to this work.

strong detergents such as sodium dodecyl sulfate that damage the remaining material and result in loss of functional matrix molecules such as bound growth factors.

Extracellular matrix (ECM) represents the secreted product of the resident cells of each tissue and organ,[9] and it is therefore logical that the ECM of each tissue and organ represents the ideal microenvironment in which organ-specific parenchymal cells can maintain their phenotype and functionality. The importance of maintaining native liver ECM structure and composition for liver regeneration was described by Vracko almost 40 years ago,[10] and more recently, the ability of liver-derived ECM to maintain hepatocyte phenotype and function in culture has been recognized.[11,12] Similarly, the ability of organ-specific ECM to support the differentiation of site-appropriate cells has been recognized for lung.[5,6,13]

It is plausible that a biologic scaffold material that contains the composition and three-dimensional structure of native liver ECM would support the viability, phenotype, and function of hepatocytes. Such technology would have a broad impact both in the clinical setting and in the scientific community. In the clinical scenario, the ability to create a functional whole-organ liver would go beyond simply treating end-stage liver failure, and could be used as a method to prevent failure in patients at risk. For the scientific community, the whole-organ technology would provide a feasible model to study liver development and hepatic maturation processes as well as a model to study complex parenchymal and nonparenchymal liver cell interactions.

The objectives of the present study were to establish an effective and minimally disruptive method for the decellularization of intact whole liver, and to compare methods for reseeding the resulting three-dimensional scaffold material with liver parenchymal cells. The methods and techniques developed in this study represent an important step toward the establishment of decellularization and recellularization criteria necessary for a successful regenerative medicine approach to liver replacement.

Materials and Methods

Animals

C57BL/6 mice (Charles River Laboratories) were used for hepatocyte isolation ($n=260$), and the isolated hepatocytes were used to evaluate cell seeding techniques, hepatocyte function, and histological studies (see below). Male Sprague-Dawley rats (250–300g; Charles River Laboratories) were used for liver harvesting and preparation of the three-dimensional liver scaffold ($n=380$) using a perfusion device to performed whole-organ decellularization and cell seeding techniques (see below). The animals were cared for in accordance with the guidelines set by the Committee on Laboratory Resources, National Institutes of Health, and Institutional Animal Care and Use Committee of University of Pittsburgh.

Donor liver harvest

Surgical plane anesthesia was induced and maintained using inhalation of 1.5%–3% of isofluorane. The abdominal cavity was opened by a ventral midline incision extending from the pubis to the xyphoid process and the animals were injected intravenously with heparin (200 units). The inferior vena cava (IVC) and the portal vein were clamped. The portal vein and IVC were then cannulated with an 18G cannula, and 5–10 mL of phosphate-buffered saline (PBS) containing heparin was injected. The diaphragm was cut to transect the superior vena cava and IVC. The liver was removed and stored in a cell culture dish filled with PBS solution. The liver was then rinsed with 10–20 mL of PBS solution containing heparin (200 units). The livers were frozen at -80°C completely immersed in PBS solution before perfusion was performed for organ decellularization.

Hepatocyte isolation

Surgical plane anesthesia was induced and mice were maintained at this plane of anesthesia by inhalation of 1.5%–3% isofluorane. Murine hepatocytes were harvested using a two-step collagenase digestion method. The isolation technique involved the cannulation and perfusion through the hepatic portal vein with calcium and magnesium-free Hanks' salt solution followed by media containing collagenase (Seromed, collagenase type CLS II) at a flow rate of 6 mL/g liver as previously described.[14] Viability was assessed by trypan blue exclusion and was routinely $>90\%$. The yield of the isolated hepatocytes was $2.0–3.0\times10^7$ cells per liver.

Whole-organ liver decellularization

The harvested livers of Sprague-Dawley rats were frozen at -80°C for at least 24 h before decellularization to aid in cell lysis. The liver was thawed at room temperature in $1\times$PBS. Decellularization was conducted by a retrograde perfusion technique at 8 mL/min, in which solutions flowed through the cannula, into the IVC, and throughout the vasculature of the liver. Livers were placed in 500 mL of 0.02% trypsin/0.05% EGTA solution at 37°C, allowing the solution to flow through the liver for 2 h. Deionized water was perfused through the liver for 15 min followed by 15 min of $2\times$PBS. The 3% Triton X-100/0.05% EGTA solution was perfused through the liver vasculature for 18–24 h with the solution being changed after 1, 4, and 16 h. A deionized water wash for 15 min followed by $2\times$PBS wash for 15 min was repeated once, followed by a deionized water wash for 30 min and $2\times$PBS wash for 30 min to aid in cellular lysis and wash any recirculating debris. The three-dimensional liver ECM was then perfused with 0.1% (v/v) peracetic acid/4% EtOH for 1 h. Acidic conditions were neutralized by PBS and deionized water washes twice for 15 min each. Decellularization was defined as (1) no visible nuclear material by histologic examination with H&E and DAPI stain; (2) DNA content of <50 ng/mg day weight, and (3) no remnant DNA with base pair length >200.[15] Terminal sterilization was accomplished by 2MRad gamma irradiation before seeding with harvested primary liver cells.

Recellularized liver graft perfusion system

The decellularized liver matrix was placed in the main chamber of customized organ chamber and a cannula was inserted into the IVC (Fig. 3e). The perfusion chamber consisted of hermetically sealed cast acrylic walls with an inside space of $1.5\times1.5\times3$ (inches), forming a reservoir filled with culture medium in which the organ was suspended. The custom chambers avoided rigid surfaces, preventing development of pressure spots and enabling sterile culture of the

recellularized grafts. The perfusion system included a peristaltic pump and bubble trap. The system was placed in an incubator for temperature control. The graft was continuously perfused through the portal veins (PVs). The medium was changed daily. The seeded cells within the culture medium were perfused into the portal vein at subphysiological flow rates of 2 mL/min to minimize shear stress and potential damage to hepatocytes.[16,17] The system was placed in a standard CO_2 (5%) cell incubator at constant temperature (37°C). The graft was continuously perfused through the portal vein at 2 mL/min. The medium was changed daily. The perfusate consisted of basal medium for hepatocyte culture: Eagle's minimal essential medium (EMEM) (Sigma), 20 ng/L Epidermol Growth Factor (EGF) (Invitrogen), 40 ng/mL hepatocyte growth factor (HGF; R&D Systems, Inc.), 10^{-8} M dexamethasone (Sigma-Aldrich), 1 mL/L insulin, human transferrin, and selenous acid supplement (ITS) (BD Bioscience), 100 U/mL penicillin, and 100 mg/L streptomycin (Invitrogen). Three methods of recellularization of the three-dimensional liver matrix were evaluated: direct parenchymal injection, continuous perfusion, and multistep infusion.

Direct parenchymal injection

About $10–50 \times 10^6$ cells (hepatocytes) suspended in culture medium were delivered through five injections of 200 μL each into different hepatic lobes of the decellularized liver matrix with a 27G needle and a 1-cc tuberculin syringe. After 40 min, the perfusate was collected, and the viability and the number of cells not retained in the liver were determined. To calculate the engraftment efficiency, the perfusate was collected and the number and viability of cells not retained in the liver was determined with a hemacytometer and trypan blue exclusion. The total number of cells retained in the decellularized liver represented the difference between the initial number of cells seeded and the number of cells present in the perfusate after seeding. The same method was applied to all three seeding methods (see below).

Continuous perfusion

About $10–50 \times 10^6$ cells (hepatocytes) suspended in the culture medium were delivered through a port located in the main chamber and the cells allowed to recirculate at a perfusion flow of 2 mL/min. After 40 min, the perfusate was collected, and the viability and the number of cells not retained in the liver were determined.

Multistep infusion

A total of $10–50 \times 10^6$ cells (hepatocytes) were infused into the circuit in multiple steps at 10–15 min intervals through a port located in the perfusion system directly in the perfused decellularized liver matrix. After 40 min, the perfusate was collected, and the viability and the number of cells not retained in the liver were determined using a hemacytometer and trypan blue exclusion. The total number of cells retained in the liver matrix was calculated as the difference between the initial number of cells seeded and the number of cells present in the perfusate at the end of seeding.

Morphologic evaluation

Decellularized/recellularized liver was fixed using 2% paraformaldehyde and 30% sucrose, and snap-frozen in liquid nitrogen for immunolabeling studies. Separate samples were fixed with glutaraldehyde in preparation for hematoxylin and eosin staining, scanning electron microscopy (SEM), and transmission electron microscopy (TEM) studies. Normal fresh rat liver was used as control. Tissues for immunolabeling and SEM were prepared and imaged as previously described.[18] Samples for SEM were sectioned into small blocks (8 mm^3), and were then fixed in 1% osmium tetroxide for 60 min. Samples were dehydrated using graded series of alcohol for 15 min each (30% ethanol, 50% ethanol, 70% ethanol, 90% ethanol, and 100% ethanol). The samples were then dried at critical point for 2 h in absolute alcohol and mounted on an aluminum stub and sputter-coated with gold before viewing under SEM. For TEM, the cells were fixed: first in 2.5% glutaraldehyde and dehydrated through graded concentrations of ethanol and embedded in Epon; Ultrathin sections of the samples were double-stained with uranyl and observed under TEM. For immunefluorescence studies, samples were cryostat sectioned ($\sim$6 μm) and placed upon glass slides. Samples were then rehydrated and permeabilized and labeled with antibodies for imaging: Rab-anti-collagen IV (BioDesign International), Rab-anti-Fibronectin (Sigma), mouse anti-laminin (kindly provided by Willi Halfter, Department of Neurobiology, University of Pittsburgh), and Rab-anti-Ki67 (Abcam) and DAPI (Vector Laboratories) were used to stain nuclei. Samples were imaged using an Olympus Provis light microscope (Brightfield, darkfield, epifluorescence DIC) or JEOL 1011CX for TEM or JEOL 9335 Field Emission Gun for SEM.

Growth factor assays

Two hundred fifty milligrams of minced rat whole liver or decellularized rat liver was suspended in $\sim$3.75 mL of urea–heparin extraction buffer. The extraction buffer consisted of 2 M urea and 5 mg/mL heparin in 50 mM Tris with protease inhibitors (protease inhibitors: 1 mM phenylmethylsulfonyl fluoride, 5 mM benzamidine, and 10 mM N-ethylmaleimide) at pH 7.4. The extraction mixture was rocked at 4°C for 20 to 24 h and then centrifuged at 12,000 *g* for 30 min. Supernatants were collected, and 6 mL of natively prepared urea–heparin extraction buffer was added to each pellet. Pellets with extraction buffer were again rocked at 4°C for 20 to 24 h, centrifuged at 12,000 *g* for 30 min, and supernatants were collected. Supernatants from first and second extractions were dialyzed against Barnstead filtered water (total of three changes of dialysis water, 80 to 100 volumes per change) in Slide-A-Lyzer Dialysis Cassettes, 3500 MWCO (Pierce). The concentration of total protein in each dialyzed extract was determined by the BCA protein assay (Pierce #23227; Pierce) following the manufacturer's protocol, and extracts were frozen in aliquots until time of assay. Concentrations of basic fibroblast growth factor (bFGF), vascular endothelial growth factor (VEGF), and HGF in urea–heparin extracts of liver samples were determined with the Quantikine Human FGF basic Immunoassay (R&D Systems # DFB50; R&D Systems), the Quantikine Rat VEGF Immunoassay (R&D Systems # DFE00; R&D Systems), and the Rat HGF ELISA Kit (B-Bridge International # K2002-1; B-Bridge International), respectively. Manufacturer's instructions were followed for all three growth factor assays. Each growth factor assay was performed in duplicate three times. Results are

reported as mean ± standard error. A one-way analysis of variance with Dunnett's comparison test was used for each growth factor analysis to test the null hypothesis that the growth factor content of the decellularized liver was no different than that of native liver. A p-value of < 0.05 was considered significant. It should be noted that growth factor assays measured the concentration of each growth factor protein and did not measure growth factor activity.

DNA quantification

DNA content was quantified using methods described previously.[19] In brief, the decellularized liver was cut into small strips and digested using Proteinase K (Invitrogen) for 24–48 h at 50°C until no visible material remained. Phenol-chloroform-isoamyl alcohol (25:24:1; Acros) was then added in equal amounts to the decellularized liver digest and centrifuged for 10 min at 10,000 *g*. The aqueous top layer containing the DNA was then removed and added to 200 μL of 3M sodium acetate solution to reduce RNA content. Ethanol was then added and the solution frozen at −80°C for at least 12 h. Ethanol was then removed, and samples were allowed to fully dry, at which point 1 × TE buffer (Invitrogen) was added. The total amount of DNA was quantified using the Picogreen DNA assay (Invitrogen) using the manufacturer's instructions.

Vascular corrosion casting

Catheterization of the infrahepatic vena cava, portal vein, hepatic artery, and bile duct was performed followed by injection of 1–4 mL polymer mixture depending on the liver size using Batson's 17 anatomic corrosion kit (Polysciences, Inc.) as recommended by the manufacturer. Polymerization took 4 h at 4°C and was followed by maceration in 1 N KOH solution or proteinase K for 8–24 h.

Functional studies

Perfusion culture medium samples were collected daily and analyzed for mouse albumin content using enzyme-linked immunosorbent assay kit as described previously (Bethyl Laboratories, Inc.).[14] Cytochrome P450-1A1/2 phase I activity is assessed by the conversion of ethoxyresorufin to resorufin by ethoxyresorufin-o-deethylase (EROD) activity. The assay was performed on cells after 4 days in culture and after an additional 3 days in culture with exposure to the prototypical CYP 1A1/2 inducer (beta-naphthoflavone). EROD assay was performed as previously described.[20] Briefly, cells were incubated for 1 h at 37°C with ethoxyresorufin solution (20 μM; Sigma-Aldrich) and salicylamide (1.5 mM; Sigma-Aldrich). The basis of the assay is that the parent compound does not fluoresce, whereas the O-deethylated species is highly fluorescent. However, the 7-OH metabolite can be rapidly metabolized through phase II enzymes within cells, and salicylamide was added to prevent conjugation of the 7-OH metabolite. After 1 h incubation, the medium was collected and frozen. All the samples were analyzed at the same time and read in triplicate. One hundred microliters of each sample was added to a 96-well plate made of white plastic specifically for the fluorescent plate reader and analyzed on a fluorimetric spectrometer (Synergy HT; Biotek Instruments, Inc.) equipped with Gen5 software at an excitation wavelength of 535 nm and an emission wavelength of 581 nm. Resorufin amount was quantified by comparing the fluorescence to a standard curve of Resorufin (Sigma-Aldrich) prepared in HMM: y [μg/mL] = 617844 * Abs + 171.23; R2 = 0.9996. Results were expressed as picomoles of product formed/min. Ammonia detoxification was evaluated after 4 and 7 days in culture. The ammonia metabolizing rate was determined after 6 h of incubation with 1 mM ammonium chloride (NH_4Cl) diluted into HMM medium. The direct colorimetric determination of ammonia was performed according to the procedure for *in vitro* quantitative determination of ammonia in whole blood (Wako Pure Chemical Industries). After deproteinization, each sample was prepared and read in triplicate by a colorimeter (uQuant; BioTek Instr., Inc.) capable of measuring absorbance at wavelengths from 560 to 600 nm. Linearity was confirmed by preparing a calibration curve in every reading. The NH3-N content is expressed as percentage of ammonia metabolized after 6 h and or pmol/min.

Statistical analyses

The mean values for cell engraftment, albumin production, and ammonia were compared by ANOVA. Fisher's protected least significant difference test was used, and a p-value of < 0.05 was considered significant. CYP1A1/2 activity was evaluated by Student's t-test.

Results

Whole-organ liver decellularization

Figure 1 shows macroscopic and microscopic images of liver before decellularization and after various steps in the decellularization process. The decellularization protocol consisted first of a freezing–thawing technique for at least 24 h to induce cellular lysis. The liver was then retrograde perfused through the IVC using 0.02% trypsin/0.05% EGTA and 3% Triton X-100/0.05% EGTA with washing and disinfection cycles for a total of 28 h (Fig. 1a). Figure 1b shows the generation of a translucent acellular liver ECM, retaining the gross anatomical features of the liver.

DNA content and remnants base pair analysis of the decellularized liver matrix

Evidence suggests that xenogeneic DNA remnants can be the cause of "inflammatory reactions" following the implantation of derived scaffolds.[19] Thus, DNA content was analyzed and gel electrophoresis confirmed that the DNA content of the decellularized liver matrix was 25.8 ± 13 ng/mg dry weight, which represents 0.47% of the DNA total content of a normal liver (5476 ± 1176 ng/mg dry weight) (Fig. 2i, note the logarithmic y-axis). Electrophoretic analysis confirmed that remaining DNA material consisted of fragments < 200 bp in length (Fig. 2j), confirming that degradation of cell contents was extensive. Histologic analysis with DAPI showed no visible nuclear material in the decellularized liver matrix (Fig. 2k).

Morphology

Histologic analysis of the decellularized liver showed the absence of cellular components compared to native liver (Fig. 1c, g). Immunolabeling characterization of the liver ECM showed the preservation of collagen IV, laminin, and fibrin-

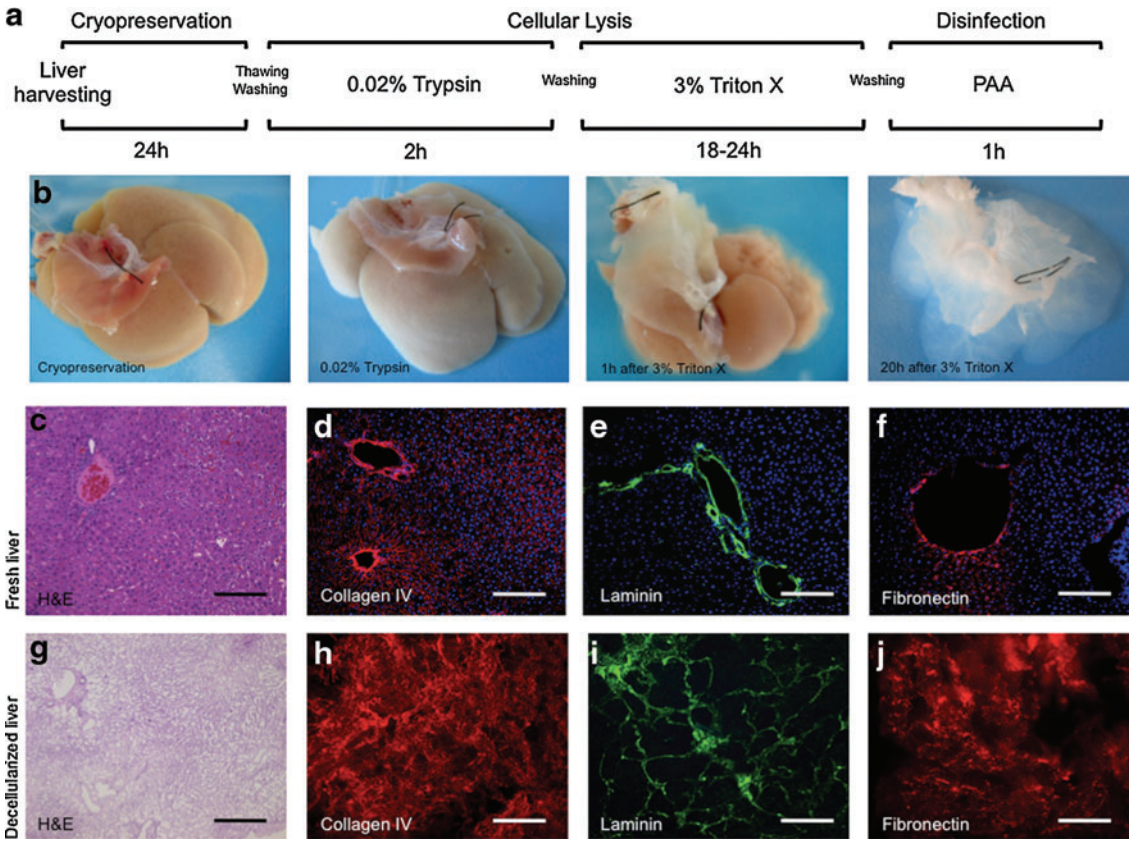

FIG. 1. Schematic representation of the sequential whole-organ decellularization protocol **(a)**. Representative macroscopic images of rat livers various steps in the decellularization process **(b)**. Histologic comparison of normal liver **(c–f)** and decellularized liver matrix **(g–j)**: hematoxylin and eosin **(c, g)**, collagen IV (red) **(d, h)**, laminin (green) **(e, i)**, and fibronectin (red) **(f, j)**. Sections were counterstained with DAPI (blue). Scale bars: 200 μm. Color images available online at www.liebertonline.com/tec

ogen, indicating a similar structural composition of the matrix to that of intact liver (Fig. 1d–f, h–j). Ultrastructural characterization of the decellularized liver matrix showed the absence of cells; the honey-comb spaces represent the footprint of hepatocyte removal (Fig. 2a, b). One important consideration in the organ decellularization process is the integrity of the collagenous capsule covering the external surface of the liver, that is, Glisson's capsule. A meticulous analysis of Glisson's capsule by both light microscopy and SEM in the present study showed complete integrity of the Glisson's capsule (Fig. 2e, f). Fresh liver from normal rats was used as control (Fig. 2c, d).

Growth factor content

The content of HGF in the decellularized liver matrix was 39 ± 1.7 ng/g dry weight and the content of bFGF was 13 ± 1 ng/g dry weight. Native liver HGF content was 72 ± 7.5 ng/g dry weight and bFGF was 34 ± 0.3 ng/g dry weight. These results show that more than 50% of HGF and ~40% of bFGF were preserved in the decellularized liver matrix compared with the native liver (Fig. 2g, h).

Vascular and bile duct morphology

Transmission electron microscope images confirmed that the basement membrane and elastin fibers of the vascular network of the decellularized liver matrix were intact (Fig. 3a), an important feature for subsequent vascular endothelialization.

In previous studies[4] it was demonstrated that only the portal and central venous system were preserved. Engineering of a complete liver graft would, however, require an intact and complete arterial system and, importantly, an intact bile drainage system. Thus, a corrosion cast of the decellularized liver matrix was created and showed the existence and preservation of the entire vascular system (portal vein, hepatic artery vasculature, central vein, and biliary tract) similar to normal liver (Fig. 3b, c).

Recellularization

To evaluate the integrity of the microvasculature and surface capsule integrity, a blue dye was perfused through the portal vein. The structural components of the vascular tree were evident and the dye flowed from the portal main vessels to the smaller capillaries, as would be expected, suggesting that the microvasculature was intact (Fig. 3d).

To facilitate cell reseeding, an organ chamber was manufactured that contains a sterile main reservoir in which the decellularized liver matrix is mounted (fig. 3e). Engraftment efficiency with the multistep infusion protocol was significantly superior $86\% \pm 5\%$ compared with direct injection

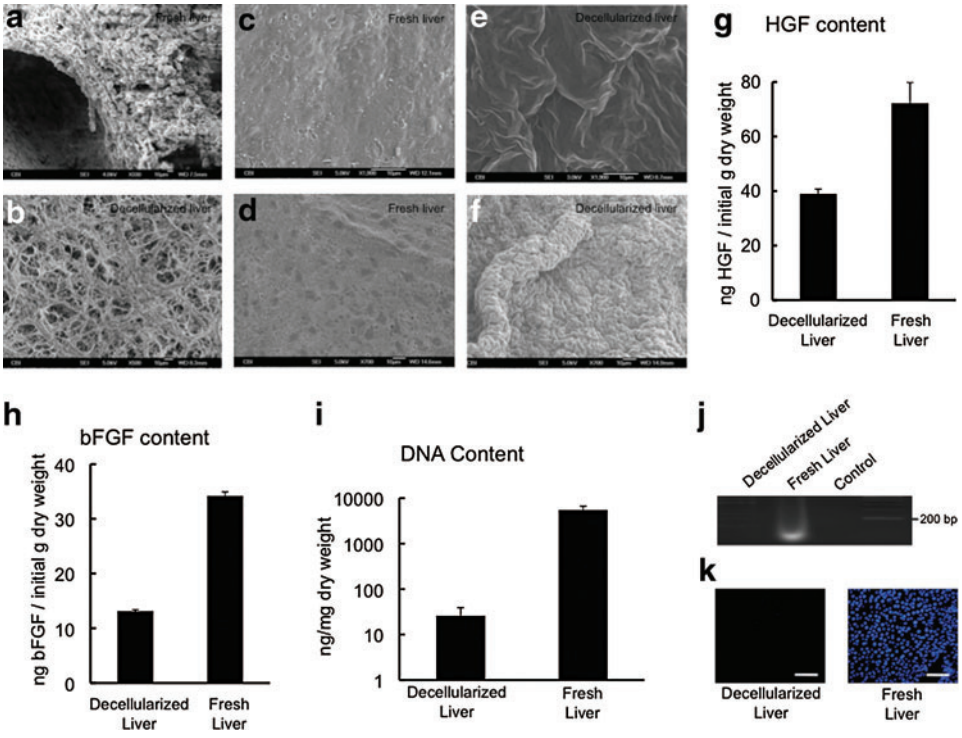

FIG. 2. Scanning electron microscopy (SEM) image showing the extracellular matrix within the parenchyma of normal liver **(a)**, and decellularized liver open spaces previously occupied by hepatic parenchymal cells **(b)**. Representative SEM images of Glisson's capsule of fresh liver **(c, d)** after liver decellularization **(e, f)** ($n=4$). Growth factor content of decellularized liver matrix and native liver, hepatocyte growth factor (HGF) **(g)**, and basic fibroblast growth factor (bFGF) **(h)** ($n=6$). DNA content of the decellularized liver matrix and native liver as determined with the PicoGreen Assay **(i, j)** ($n=6$) the presence of intact nuclear material was evaluated by staining the decellularized liver and native liver using 4′,6-diamidino-2-phenylindole (DAPI) **(k)** ($n=3$). Scale bars: 10 μm **(a–f)**. Color images available online at www.liebertonline.com/tec

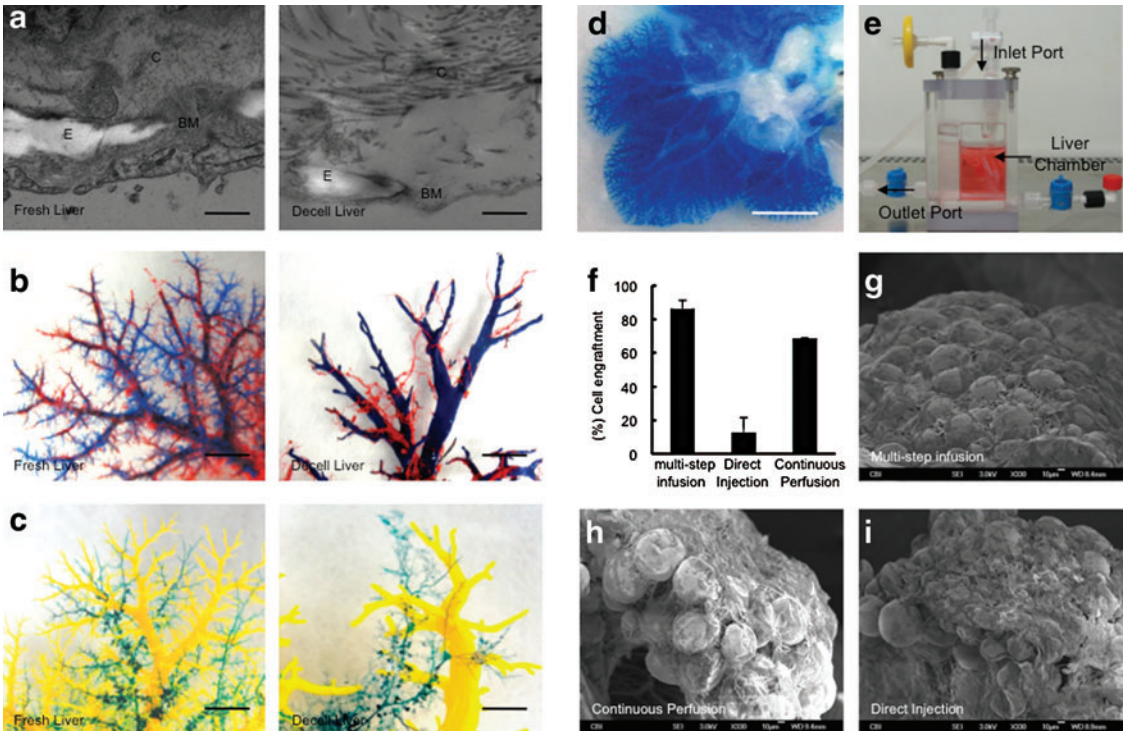

FIG. 3. The decellularized liver matrix preserves entire vascular bed and bile ducts. TEM images larger vessels of native liver and decellularized liver **(a)**. Representative photographs of decellularized left lateral and median lobes of rat liver, with the vascular tree visible. A corrosion cast model of native liver and the decellularized liver shows portal (blue), arterial (red) vasculature and venous vasculature (yellow), and bile duct (green) **(b, c)**. Representative photographs of visible microvascular tree **(d)**, after perfusion with blue dye in the organ chamber **(e)**. Cell engraftment efficiency percentage in three different cell-seeding techniques ($p<0.0001$) **(f)** ($n=3$). SEM micrographs of recellularized liver graft after 4 days in culture using three different cell-seeding techniques **(g–i)**. Scale bars: 5 μm **(a)**, 1 mm **(b, c)**, 5 mm **(d)**, 10 μm **(g–i)**. E, elastin; C, collagen; BM, basement membrane. Error bars represent SE ($n=3$). Color images available online at www.liebertonline.com/tec

12.6%±9% ($p<0.0001$) or pump perfusion 69%±0.5% ($p=0.0172$) methods (Fig. 3f). SEM showed that hepatocytes engrafted around the larger vessels, repopulating the surrounding parenchymal area (Fig. 3g–i).

The engraftment efficiency and the capacity to culture cells within the decellularized liver matrix in the organ chamber provide the ability to evaluate cell survival and proliferation, and to characterize liver-specific metabolic function *in vitro*. The amount of immunostaining of albumin in engrafted hepatocytes was similar to that in normal livers (Fig. 4a–d); however, decellularized livers reseeded with hepatocytes using the pump perfusion technique showed less albumin expression.

To assess the cell proliferation ability of the seeded heatocytes using the three different methods in the decellularized liver matrix, Ki67 staining was performed and showed that 3%±0.6% of the cells seeded using the multistep infusion seeding method were positive for Ki67 antibody,

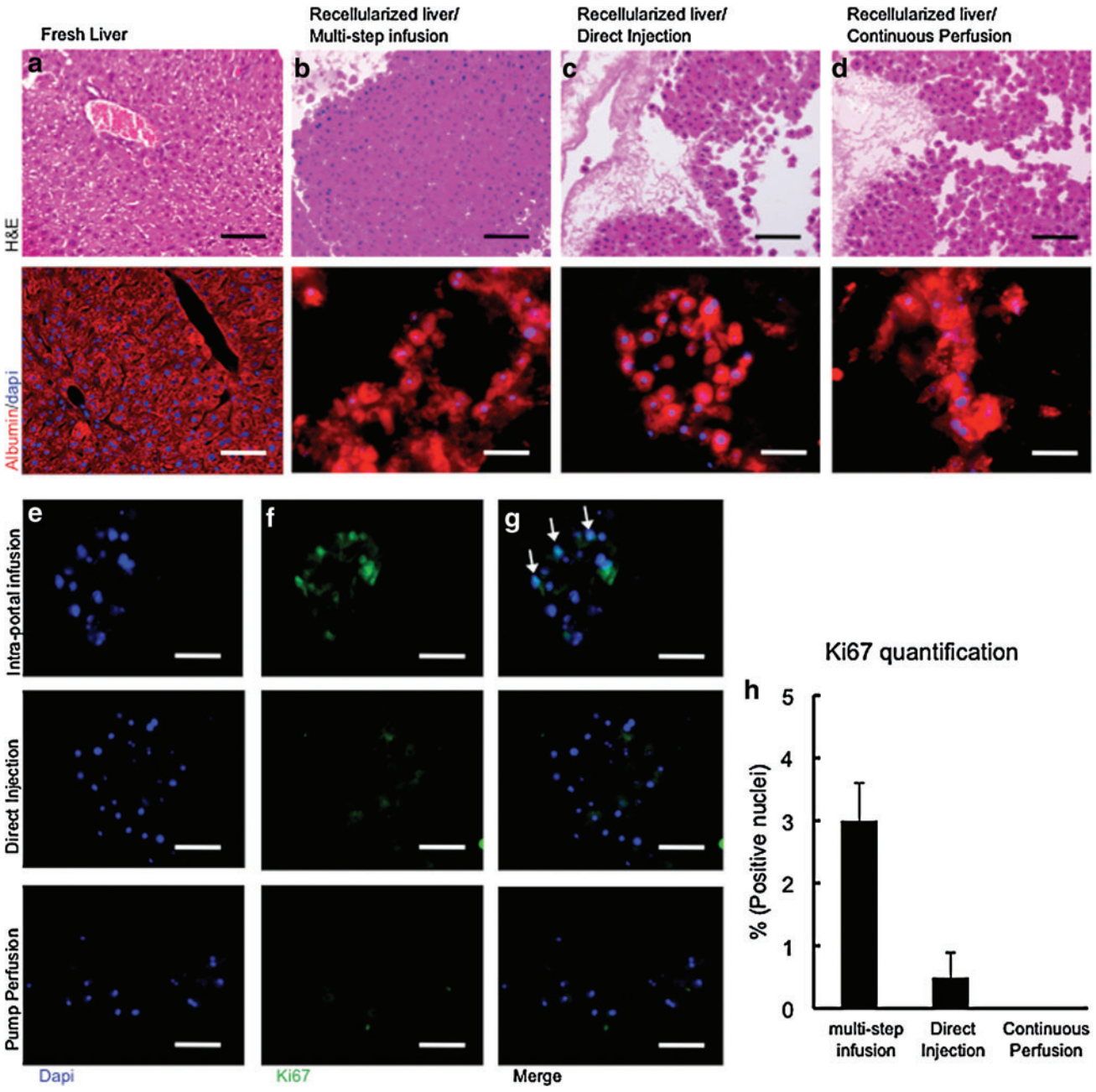

FIG. 4. Repopulation of decellularized liver matrix with adult hepatocytes. Immunohistochemical staining of native liver **(a)** and the recellularized liver grafts using three different cell-seeding techniques **(b–d)**: H&E (first row) and albumin (red) (second row). Sections were counterstained with DAPI (blue). Ki67 staining of recellularized liver grafts using three different cell-seeding techniques: arrows indicate positive cells. DAPI was used as counterstain of the same sections **(e)**. Ki67-staining (green) **(f)**. Merge images of the three different cell-seeding techniques **(g)**. Ki67-positive cell percentage in recellularized liver grafts on day 4 of culture **(h)**. Scale bars: 100 μm **(a–d)**, 50 μm **(e–g)**. Color images available online at www.liebertonline.com/tec

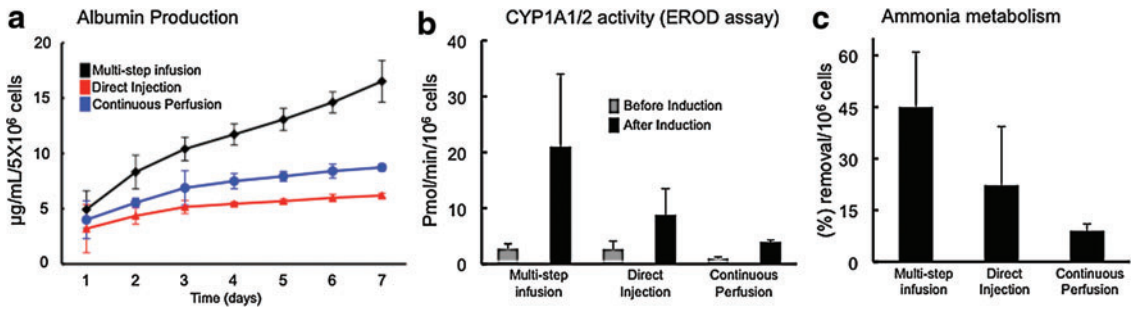

FIG. 5. Hepatic function of the recellularized liver matrix. Albumin synthesis using three different cell-seeding techniques **(a)**. Intraportal multistep infusion versus direct injection ($p=0.052$); intraportal multistep infusion versus pump perfusion ($p=0.08$); direct injection versus pump perfusion ($p=0.876$); ($n=4$). To assess liver-specific cytochrome P450 metabolic activity of the seeded hepatocytes, cytochrome P450-1A1/2 phase I activity was measured by ethoxyresorufin-o-deethylase (EROD) activity **(b)**. Intraportal multistep infusion ($p=0.149$); direct injection ($p=0.115$); pump perfusion ($p=0.1087$); $n=3$. Ammonia metabolizing activity on day 4 of culture of the recellularized liver grafts **(c)**. Intraportal multistep infusion versus direct injection ($p=0.126$); intraportal multistep infusion versus pump perfusion ($p=0.03$); direct injection versus pump perfusion ($p=0.3365$); $n=3$. Color images available online at www.liebertonline.com/tec

showing that the conditions provided by the liver matrix are adequate for viable and proliferating seeded hepatocytes (Fig. 4e–h).

To evaluate the metabolic activity of engrafted hepatocytes in the decellularized liver matrix, albumin production, CYP1A1/2 activity, and ammonia clearance ability were quantified. The cumulative albumin production at 7 days of culture was $16.5\pm1.8\,\mu g/mL$ for the multistep infusion technique and 6 ± 0.2 and $8.7\pm0.3\,\mu g/mL$ for the direct injection and continuous perfusion technique, respectively (Fig. 5a). These results showed greater ability to produce albumin when hepatocytes were seeded in the decellularized liver matrix using the multistep infusion technique than the other two recellularization techniques.

Hepatocytes seeded using the three different techniques showed inducible hepatic CYP 1A1/1A2-mediated EROD activity. CYP 1A1/2 EROD activity for multistep infusion technique was $2.8\pm0.8\,pmol/min/million$ cells before induction and $21\pm13\,pmol/min/million$ cells after induction (Fig. 5b). For the direct injection seeding technique, the CYP1A1/2 EROD activity was $2.7\pm1.4\,pmol/min/million$ cells before induction and $8.8\pm4.7\,pmol/min/million$ cells after induction (Fig. 5b). The continuous perfusion technique results showed $1.05\pm0.2\,pmol/min/million$ cells before induction and $3.95\pm0.2\,pmol/min/million$ cells after induction (Fig. 5b). EROD activity was superior when the multistep infusion was used (Fig. 5b). Ammonia clearance ability was investigated in the three seeding techniques (Fig. 5c) and no significant difference was found within the groups; however, the multistep infusion technique showed higher levels of ammonia removal (Fig. 5c).

Discussion

The present study describes a minimally disruptive whole-organ decellularization protocol that produces a three-dimensional liver matrix suitable for supporting functional hepatocytes, and a comprehensive characterization of the decellularized liver matrix shows maintenance of the hepatic matrix ultrastructure and preservation of representative growth factors such as bFGF and HGF. Importantly, a comparison of three methods for reintroducing cells to the matrix identified a multistep perfusion technique that results in 90% grafting efficiency.

The results of the present study not only confirm the concept of whole-organ decellularization, as previously shown,[5–7,13,21] but also provide new findings not reported in previous studies that will be important for clinical translation of this regenerative medicine approach for liver replacement. First, thorough decellularization can be accomplished in $\sim48\,h$ without the use of harsh detergents such as sodium dodecyl sulfate. Second, growth factor content can be preserved within the matrix scaffold at 30%–50% of the native tissue. Third, decellularization was quantified by stringent and conservative criterion showing absolute amounts of residual DNA and not just percent decrease, and that any residual DNA consisted only of lengths no $>200\,bp$; stated differently, very thorough decellularization was accomplished. As shown in previous studies, DNA fragments with $<300\,bp$ in length have shown no significant inflammatory reactions in several commercially available ECM products and ECM scaffold materials produced in the laboratory.[19] Fourth, the biliary network was shown to be intact, along with the vascular structures. Fifth, Glisson's capsule was shown to be intact, an important feature because of anticipated future clinical applications in which hemorrhage after connection to an *in vivo* vascular supply would be problematic. Finally, systematic comparison of three different reseeding methods showed that a multistep strategy provides the greatest seeding efficiency and the presence of functional hepatocytes.

One of the main limiting factors in the advancement of liver tissue engineering is the lack of an ideal transplantable scaffold that has all the necessary microstructural and extracellular cues for cell attachment, differentiation, functioning, and vascularization for oxygen and nutrient transport.[14,22,23] Thus, the ability to create a transplantable liver scaffold is an important advancement in proof of concept. Whole-organ decellularization has been recently reported for different organs, including liver[4–7,24]; however, *in vivo* implantation has been limited to a few hours due to problems such as hemorrhage and thrombosis. The method for whole-liver decellularization reported herein directly addresses some of the issue that will determine ultimate clinical success.

The ECM in the developing liver has dynamic structural and functional features that mature with age and which directly affect the fate and gene expression of hepatoblasts.[25] The various growth factors and chemo attractants are immobilized by ECM components through disulfide bonds.[26,27] Thus, the well-defined ECM provided in the adult liver could potentially facilitate and guide the developmental pathway for full hepatic maturation of fetal liver cells or embryonic and/or induced pluripotent stem cells. Organ decellularization could potentially become a tool for stem cell differentiation and maturation to eventually engineer autologous liver grafts for transplantation.[28] Studies with decellularized lung show the important role played by microenvironmental ECM signals for determination of stem cell differentiation fate.[5,13] The growth factor content in the decellularized liver matrix of the present study showed that this decellularization protocol can preserve up to half of the HGF and bFGF content of the normal liver. HGF and bFGF are essential growth factors in angiogenesis and hepatic differentiation.[29,30] VEGF content was below detection amounts in the current decellularized liver matrix.

Eventual replacement of the entire sophisticated liver architecture will require addition of liver nonparenchymal cells, especially liver sinusoidal and macrovascular endothelial cells, to vascularize the entire graft and prevent thrombosis caused by direct exposure of the collagenous basement membrane to the circulation. Moreover, strategies to solve bile drainage must be developed; however, the fact that the biliary tract is preserved by the present decellularization method maintains the possibility to reconstitute it with biliary epithelial cells.

Different techniques were investigated to seed primary hepatocytes in the decellularized liver matrix. The multistep perfusion technique produced $\sim$90% cell engraftment efficiency. The perfusion technique showed deposition of the primary hepatocytes within the parenchymal space and occasionally in the vessels. A possible explanation for this result is the lack of the endothelial cell barrier, abundant empty parenchymal space, and the openings within the collagen-rich basement membrane structure of the vasculature due to the mechanical pressure of the perfusion flow. After engraftment, hepatocytes showed viability, albumin expression, and secretion abilities and metabolic activity in perfusion for up to 7 days. Differences in outcomes within the cell seeding techniques may be the result of different mechanical stress of each seeding technique.

Ongoing studies are directed toward complete re-endothelialization, biliary tract reconstruction, and hepatic differentiation and reconstitution using a variety of stem cells and differentiated cells. Addition of nonparenchymal liver cells and transplantation in special liver-reconditioned animal models may enhance the reconstitution and regeneration of the decellularized/recellularized liver graft *in vivo*. Thus, the possible *in vivo* production of liver grafts using decellularized/recellularized liver graft ultimately as an *in vivo* model for liver regeneration and development is envisioned. This technology could have a notable impact in the clinical setting as the whole-organ grafts could be used to treat patients with congenital enzymatic liver diseases, possibly allowing the repopulation of the patient liver with healthy hepatocytes. These grafts could change living-donor liver transplantation in that left-lateral grafts—currently not deemed sufficient for adult recipients—could be sufficient to support the patient when performed in tandem with the hepatic support provided by the liver grafts. This system may prove to be a superior liver cell culture system for pharmacology, drug discovery, and toxicologic studies of a compound in human liver grafts *in vitro* prior the exposure to the whole body, by providing a natural environment for the hepatocytes. Such utility potentially translates into reduced costs and time in drug development, and less harmful patient exposure in clinical trials. Additionally, the whole-organ liver would provide a feasible model to study liver development and ultimately as an auxiliary liver graft for transplantation.

In summary, the data presented herein support this scaffold plus cell-based regenerative medicine strategy for functional liver replacement. The resultant liver matrix scaffold has all the obvious necessary microstructure and extracellular cues for cell attachment, differentiation, functioning, and vascularization.

Acknowledgments

This work was supported by grants from the Commonwealth of Pennsylvania (AR053603 to S.B.) and NIH (K99DK083556 to A.S.-G.). We would like to thank the support of the American Liver Foundation to A.S.-G. and the Research Fellowship of the Japan Society for the Promotion of Science for young scientist to K.F.

Disclosure Statement

The authors declare no competing financial interests.

References

1. Klein, A.S., Messersmith, E.E., Ratner, L.E., Kochik, R., Baliga, P.K., and Ojo, A.O. Organ donation and utilization in the United States, 1999–2008. Am J Transplant **10,** 973, 2010.
2. Soltys, K.A., Soto-Gutierrez, A., Nagaya, M., Baskin, K.M., Deutsch, M., Ito, R., Shneider, B.L., Squires, R., Vockley, J., Guha, C., Roy-Chowdhury, J., Strom, S.C., Platt, J.L., and Fox, I.J. Barriers to the successful treatment of liver disease by hepatocyte transplantation. J Hepatol **53,** 769, 2010.
3. Kidambi, S., Yarmush, R.S., Novik, E., Chao, P., Yarmush, M.L., and Nahmias, Y. Oxygen-mediated enhancement of primary hepatocyte metabolism, functional polarization, gene expression, and drug clearance. Proc Natl Acad Sci U S A **106,** 15714, 2009.
4. Uygun, B.E., Soto-Gutierrez, A., Yagi, H., Izamis, M.L., Guzzardi, M.A., Shulman, C., Milwid, J., Kobayashi, N., Tilles, A., Berthiaume, F., Hertl, M., Nahmias, Y., Yarmush, M.L., and Uygun, K. Organ reengineering through development of a transplantable recellularized liver graft using decellularized liver matrix. Nat Med **16,** 814, 2010.
5. Petersen, T.H., Calle, E.A., Zhao, L., Lee, E.J., Gui, L., Raredon, M.B., Gavrilov, K., Yi, T., Zhuang, Z.W., Breuer, C., Herzog, E., and Niklason, L.E. Tissue-engineered lungs for *in vivo* implantation. Science **329,** 538, 2010.
6. Ott, H.C., Clippinger, B., Conrad, C., Schuetz, C., Pomerantseva, I., Ikonomou, L., Kotton, D., and Vacanti, J.P. Regeneration and orthotopic transplantation of a bioartificial lung. Nat Med **16,** 927, 2010.
7. Ott, H.C., Matthiesen, T.S., Goh, S.K., Black, L.D., Kren, S.M., Netoff, T.I., and Taylor, D.A. Perfusion-decellularized matrix: using nature's platform to engineer a bioartificial heart. Nat Med **14,** 213, 2008.

8. Wainwright, J.M., Czajka, C.A., Patel, U.B., Freytes, D.O., Tobita, K., Gilbert, T.W., and Badylak, S.F. Preparation of cardiac extracellular matrix from an intact porcine heart. Tissue Eng Part C Methods **16,** 525, 2010.
9. Badylak, S.F., Freytes, D.O., and Gilbert, T.W. Extracellular matrix as a biological scaffold material: structure and function. Acta Biomater **5,** 1, 2009.
10. Vracko, R. Basal lamina scaffold-anatomy and significance for maintenance of orderly tissue structure. Am J Pathol **77,** 314, 1974.
11. Sellaro, T.L., Ranade, A., Faulk, D.M., McCabe, G.P., Dorko, K., Badylak, S.F., and Strom, S.C. Maintenance of human hepatocyte function *in vitro* by liver-derived extracellular matrix gels. Tissue Eng Part A **16,** 1075, 2010.
12. Sellaro, T.L., Ravindra, A.K., Stolz, D.B., and Badylak, S.F. Maintenance of hepatic sinusoidal endothelial cell phenotype *in vitro* using organ-specific extracellular matrix scaffolds. Tissue Eng **13,** 2301, 2007.
13. Cortiella, J., Niles, J., Cantu, A., Brettler, A., Pham, A., Vargas, G., Winston, S., Wang, J., Walls, S., and Nichols, J.E. Influence of acellular natural lung matrix on murine embryonic stem cell differentiation and tissue formation. Tissue Eng Part A **16,** 2565, 2010.
14. Soto-Gutierrez, A., Navarro-Alvarez, N., Rivas-Carrillo, J.D., Tanaka, K., Chen, Y., Misawa, H., Okitsu, T., Noguchi, H., Tanaka, N., and Kobayashi, N. Construction and transplantation of an engineered hepatic tissue using a polyaminourethane-coated nonwoven polytetrafluoroethylene fabric. Transplantation **83,** 129, 2007.
15. Crapo, P.M., Gilbert, T.W., and Badylak, S.F. An overview of tissue and whole organ decellularization processes. Biomaterials **32,** 3233, 2011.
16. Torii, T., Miyazawa, M., and Koyama, I. Effect of continuous application of shear stress on liver tissue: continuous application of appropriate shear stress has advantage in protection of liver tissue. Transplant Proc **37,** 4575, 2005.
17. Tilles, A.W., Baskaran, H., Roy, P., Yarmush, M.L., and Toner, M. Effects of oxygenation and flow on the viability and function of rat hepatocytes cocultured in a microchannel flat-plate bioreactor. Biotechnol Bioeng **73,** 379, 2001.
18. Straub, A.C., Clark, K.A., Ross, M.A., Chandra, A.G., Li, S., Gao, X., Pagano, P.J., Stolz, D.B., and Barchowsky, A. Arsenic-stimulated liver sinusoidal capillarization in mice requires NADPH oxidase-generated superoxide. J Clin Invest **118,** 3980, 2008.
19. Gilbert, T.W., Freund, J.M., and Badylak, S.F. Quantification of DNA in biologic scaffold materials. J Surg Res **152,** 135, 2009.
20. Wen, Y.H., Sahi, J., Urda, E., Kulkarni, S., Rose, K., Zheng, X., Sinclair, J.F., Cai, H., Strom, S.C., and Kostrubsky, V.E. Effects of bergamottin on human and monkey drug-metabolizing enzymes in primary cultured hepatocytes. Drug Metab Dispos **30,** 977, 2002.
21. Yarmush, M.L., Dunn, J.C., and Tompkins, R.G. Assessment of artificial liver support technology. Cell Transplant **1,** 323, 1992.
22. Navarro-Alvarez, N., Soto-Gutierrez, A., Chen, Y., Caballero-Corbalan, J., Hassan, W., Kobayashi, S., Kondo, Y., Iwamuro, M., Yamamoto, K., Kondo, E., Tanaka, N., Fox, I.J., and Kobayashi, N. Intramuscular transplantation of engineered hepatic tissue constructs corrects acute and chronic liver failure in mice. J Hepatol **52,** 211, 2010.
23. Soto-Gutierrez, A., Navarro-Alvarez, N., Yagi, H., Nahmias, Y., Yarmush, M.L., and Kobayashi, N. Engineering of an hepatic organoid to develop liver assist devices. Cell Transplant **19,** 815, 2010.
24. Shupe, T., Williams, M., Brown, A., Willenberg, B., and Petersen, B.E. Method for the decellularization of intact rat liver. Organogenesis **6,** 134, 2010.
25. Stamatoglou, S.C., Enrich, C., Manson, M.M., and Hughes, R.C. Temporal changes in the expression and distribution of adhesion molecules during liver development and regeneration. J Cell Biol **116,** 1507, 1992.
26. Pekkari, K., and Holmgren, A. Truncated thioredoxin: physiological functions and mechanism. Antioxid Redox Signal **6,** 53, 2004.
27. Agrawal, V., Johnson, S.A., Reing, J., Zhang, L., Tottey, S., Wang, G., Hirschi, K.K., Braunhut, S., Gudas, L.J., and Badylak, S.F. Epimorphic regeneration approach to tissue replacement in adult mammals. Proc Natl Acad Sci U S A **107,** 3351, 2010.
28. Soto-Gutierrez, A., Yagi, H., Uygun, B.E., Navarro-Alvarez, N., Uygun, K., Kobayashi, N., Yang, Y.G., and Yarmush, M.L. Cell delivery: from cell transplantation to organ engineering. Cell Transplant **19,** 655, 2010.
29. Basma, H., Soto-Gutierrez, A., Yannam, G.R., Liu, L., Ito, R., Yamamoto, T., Ellis, E., Carson, S.D., Sato, S., Chen, Y., Muirhead, D., Navarro-Alvarez, N., Wong, R.J., Roy-Chowdhury, J., Platt, J.L., Mercer, D.F., Miller, J.D., Strom, S.C., Kobayashi, N., and Fox, I.J. Differentiation and transplantation of human embryonic stem cell-derived hepatocytes. Gastroenterology **136,** 990, 2009.
30. Soto-Gutierrez, A., Kobayashi, N., Rivas-Carrillo, J.D., Navarro-Alvarez, N., Zhao, D., Okitsu, T., Noguchi, H., Basma, H., Tabata, Y., Chen, Y., Tanaka, K., Narushima, M., Miki, A., Ueda, T., Jun, H.S., Yoon, J.W., Lebkowski, J., Tanaka, N., and Fox, I.J. Reversal of mouse hepatic failure using an implanted liver-assist device containing ES cell-derived hepatocytes. Nat Biotechnol **24,** 1412, 2006.

Address correspondence to:
Stephen F. Badylak, D.V.M., Ph.D., M.D.
McGowan Institute for Regenerative Medicine
University of Pittsburgh
450 Technology Drive, Suite 300
Pittsburgh, PA 15219

E-mail: badylaks@upmc.edu

Alejandro Soto-Gutierrez, M.D., Ph.D.
Transplantation Section
Department of Surgery
Children's Hospital of Pittsburgh
Center for Innovative Regenerative Therapies
University of Pittsburgh
3511 Rangos Research Building 530 45th St.
Pittsburgh, PA 15201

E-mail: sotogutierreza@upmc.edu

Received: December 1, 2010
Accepted: March 3, 2011
Online Publication Date: April 19, 2011